coatings

MDPI

Article

Plasma-Deposited Organosilicon Hydrophobic Coatings on Cellulosic Materials for Wet Packaging Applications

Jacopo Profili [1,†], Sara Babaei [1,†], Mariam Al Rashidi [1], Annie Dorris [2], Siavash Asadollahi [3], Andranik Sarkissian [3] and Luc Stafford [1,*]

[1] Département de Physique, Université de Montréal, 1375 Ave Thérèse-Lavoie-Roux, Montréal, QC H2V 0B3, Canada
[2] FPInnovations, 570 Boul. Saint-Jean, Pointe-Claire, QC H9R 3J9, Canada
[3] Plasmionique, 1650 Lionel-Boulet, Varennes, QC J3X 1S2, Canada
* Correspondence: luc.stafford@umontreal.ca
† These authors contributed equally to this work.

Abstract: Non-toxic organosilicon coatings with hydrophobic properties were deposited on Kraft paper films using atmospheric-pressure dielectric barrier discharge. In order to assess the applicability of the plasma-deposited coating in the food packaging industry, its stability in different liquids (i.e., food simulants) was studied. Chemical analyses reveal that the food simulants, namely, de-ionized water, acetic acid, ethanol, and heptane, do not significantly alter the chemical composition or the hydrophobicity of the coatings. Based on inductively coupled plasma-optical emission spectroscopy analyses, the amount of Si released from the plasma-deposited coating is less than that typically detected in tap water. Overall, the results obtained suggest that hydrophobic plasma-deposited organosilicon coatings have great potential for use in food and wet packaging applications, especially considering their environmentally friendly character.

Keywords: organosilicon coating; dielectric barrier discharge; wet packaging; compound migration; cellulose

Citation: Profili, J.; Babaei, S.; Al Rashidi, M.; Dorris, A.; Asadollahi, S.; Sarkissian, A.; Stafford, L. Plasma-Deposited Organosilicon Hydrophobic Coatings on Cellulosic Materials for Wet Packaging Applications. *Coatings* **2023**, *13*, 924. https://doi.org/10.3390/coatings13050924

Academic Editors: Ruchir Priyadarshi, Swarup Roy, Shiv Dutt Purohit and Tabli Ghosh

Received: 13 February 2023
Revised: 2 May 2023
Accepted: 4 May 2023
Published: 15 May 2023

1. Introduction

Paper and its derivatives, such as paperboards and linerboards, are currently the preferred packaging materials due to their bio-based, green, and sustainable nature, as well as their good mechanical strength, high flexibility, and low cost. However, these materials are highly sensitive to moisture and can be easily damaged by water [1], which limits their use in industrial applications such as packaging [2], food storage [3], medicines, printing [4], and microfluidic or bioassay devices [5]. Recently, great research efforts have been put towards tuning the liquid resistance of renewable and biodegradable cellulose-based resources, leading to the development of several processes (e.g., bulk modification, surface treatment, and fiber structuration) and additives that can be used to enhance the durability of cellulosic substrates in wet environments [6,7]. Researchers have been particularly interested in increasing the hydrophobicity of these substrates [8–10]. Most hydrophobization techniques currently used in industrial applications rely on internal or surface sizing agents [11]. However, novel techniques make use of micro/nanoengineering processes to enhance the surface hydrophobicity of cellulosic materials [12]. Graft polymerization is one such technique that has been widely applied to the chemical modification of cellulose surfaces [13]. By grafting vinyl monomers with long paraffin chains on the surface of cellulose using direct irradiation, Takács et al. [14] succeeded in reducing the swelling of cellulosic fibers and improving their water droplet uptake. Surface-initiated atom transfer radical polymerization (ATRP) is another technique that has been used to modify pulp and cellulose fibers by grafting with different compounds (e.g., polystyrene) [15].

Recently, plasma processes have shown great potential for tuning the wetting properties of various cellulosic materials [9,16–25]. In contrast to the chemical techniques, these processes are carried out in a dry and low-temperature medium, which reduces the risk of physical and thermal damage for heat-sensitive materials such as cellulose [26]. Moreover, plasma processes are eco-friendly and cost-effective, as they do not require solvents or large amounts of chemicals [27]. In a study conducted by Blanchard et al. [18], low-pressure discharges with hexamethyldisiloxane (HMDSO) precursors were used to prepare hydrophobic thin plasma polymer films that can enhance the water repellency of hydrophilic substrates such as wood. Similarly, Levasseur et al. [9,22] were able to deposit hydrophobic polymer films onto wood surfaces using plane-to-plane dielectric barrier discharge at atmospheric pressure. Although the films deposited by He/HMDSO and Ar/C_3F_8 plasmas enhanced the hydrophobicity of wood, the ones deposited by the N_2/C_3F_8 plasma had no appreciable effect on hydrophobicity. This shows that the carrier gas plays an important role in the plasma polymerization process [9]. Other studies confirm that plasma polymerization of Si- and F-based precursors can effectively improve the water repellency of cellulosic surfaces [16,17,21,24,25,28–33]. Considering that the nanometric modifications induced by the plasma affect only the extreme surface of the fibers (i.e., a few nm depth), the light weight and recyclability of cellulose-based materials should not be compromised by plasma surface modification. In light of these advantages, plasma is currently considered a promising new method for enhancing the surface hydrophobicity of cellulose-based fibrous and porous materials [34,35].

In order to ensure product safety, the plasma-processed materials used in the food and packaging industries must be carefully designed such that the migration of compounds, i.e., their diffusion from the food-contact layer (coating) to the food surface [36], is limited [36,37], irrespective of the packaging conditions (e.g., temperature, contact duration, and degree of solvent stirring [38,39]). To prevent the migration of compounds from cellulosic packaging materials such as paper and paperboards, these materials are often coated with waxes or polymeric films, including polysaccharide, poly(lactic acid), poly(butylene succinate), poly(butylene adipate-co-terephthalate), and poly(ε-caprolactone) films, among others [40]. Depending on the targeted application, the coatings are designed in such a way that they enhance the barrier (oxygen, aroma, and oil) properties of the cellulosic substrates as well as their water repellency. Moreover, they are used to ameliorate the surface and gloss finish, stability, printability, readability, and antimicrobial performance of the packaging material [40]. Although numerous studies have been conducted on the contamination of food products with vinyl chloride monomer (VCM) and polyvinyl chloride (PVC) plasticizers [41–45], few studies are available regarding compound migration from plasma-processed coatings on paper and paper products [18]. In this regard, the research presented herein focuses on the end-user properties of plasma-processed paper surfaces. Specifically, the migration of compounds from a hydrophobic organosilicon coating deposited on Kraft paper is assessed. Compared to other coating materials, organosilicon is more advantageous due to its transparency, hardness, and compatibility with organic compounds [46]. Moreover, organosilicon coatings can effectively crosslink with different types of substrates due to their high organic content [47], and they can enhance the heat, corrosion, and wear resistance of substrates [48]. Herein, the coating is prepared by polymerization of HMDSO using atmospheric-pressure dielectric barrier discharge (DBD), a non-destructive surface engineering technique. HMDSO is selected as a precursor due to its non-toxic nature as well as the excellent properties of its plasma polymers, such as good hardness [49], low gas permeability [50], and high resistance to chemicals [51]. Notably, the same method was applied in a previous study, wherein we showed that the plasma-deposited organosilicon coating significantly reduces the water repellency of a cellulosic substrate [52]. Herein, the migration of compounds from the coating is tested by immersion and shaking in different food simulant (FS) solutions approved by the Food and Drug Administration (FDA, Silver Spring, MD, USA), under FDA-specified conditions [53]. Fourier transform infrared (FTIR) spectroscopy, wettability, and scanning electron microscopy (SEM) analyses of the coatings

are conducted before and after immersion to examine their chemical stability, hydrophobicity, and morphology. Meanwhile, the solutions are analyzed by inductively coupled plasma-optical emission spectroscopy (ICP-OES) to measure the amount of silicon migrated from the coatings to the food stimulants, if any.

2. Materials and Methods

2.1. Plasma Deposition Conditions

The 100-µm-thick handsheets used as cellulosic substrates in this study were made of bleached, refined thermochemical Kraft pulp, and they were provided by FPInnovations. The porosity of these handsheets was analyzed at the manufacturing company (FPInnovations, Pointe-Claire, QC, Canada) using mercury intrusion porosimetry. This technique is generally used to determine the diameter distribution, volume, and surface area of pores in a substrate by forcing mercury into the pore structure of a vacuumed sample. The results obtained show that the Kraft papers used herein have a total porosity of 58% and an average pore size of 2.3 µm. Organosilicon coatings were deposited on the handsheet substrates using a plane-to-plane DBD housed in a vacuum chamber. The discharge was ignited by applying a sinusoidal voltage (2 kV_{pp}, 20 kHz) between two alumina plate electrodes (6.5 cm × 5.5 cm, 635 µm thickness) coated with metalized paint (Pt-Ag alloy). The gap between the two electrodes was kept at 1 mm using two glass slides. More details on the experimental setup for plasma deposition can be found in previous studies [54,55]. To conduct an experiment, the Kraft paper substrate was first fixed to the lower electrode using Kapton tape (Bertech, Torrance, CA, USA). The tape was applied on all sides of the substrate to prevent any gas diffusion from the edges. Subsequently, the chamber was pumped down to reduce impurities, and then it was filled with helium to atmospheric pressure. During the plasma deposition process, atmospheric pressure was maintained in the chamber by gentle pumping. A 4.5 L/min flow of He gas was used to carry the HMDSO vapors (120 g/h; Sigma Aldrich, Burlington, MA, USA) into the reactor through a diffuser located on one side of the discharge cell. Based on the current-voltage waveforms, the discharge was operated in a glow-like homogeneous regime [54–56].

2.2. Immersion Conditions

In order to evaluate the stability of the organosilicon coating deposited on Kraft paper, the plasma-treated samples were immersed and shaken in different food stimulants under variable time, temperature, and shaking rate conditions (Table 1). Detailed analyses of the FS solutions and paper samples were conducted before and after immersion to assess the chemical safety of the packaging material, as per the requirements of the Health Products and Food Branch (HPFB) [57]. Aqueous ethanol was chosen as a fatty food simulant, and the samples were immersed in a 95% v/v ethanol solution, which mimics highly alcoholic and fatty foods [58]. In addition, extractions were carried out in de-ionized (DI) water, 3% acetic acid solution, and heptane, all of which are admissible food simulants by the FDA. The extraction conditions were selected based on the potential use of the plasma-deposited Kraft paper films in disposable food packaging products (e.g., paper cups, paper plates, food containers, etc.). For example, hot beverages such as tea, hot chocolate, and coffee are regularly served at temperatures between 60 and 85 °C [59], whereas the preferred temperature for cold beverages falls in the range of 4–20 °C. Therefore, the investigated temperatures in this work were 23 °C (room temperature), 40 °C, and 65 °C. Notably, the maximal speed and temperature of the incubator (Ecotron; INFORS HT, Montreal, QC, Canada) used to conduct extraction experiments were 140 rpm and 65 °C, respectively.

Table 1. Conditions applied during the extraction experiments.

Variable	Time (h)	Temperature (°C)	RPM * (min^{-1})
Parametric study 1	0.5 3 16 24	Constant (40)	Constant (50)
Parametric study 2	Constant (3)	23 40 65	Constant (50)
Parametric study 3	Constant (3)	Constant (65)	50 140

* RPM is revolutions per minute.

2.3. Characterization of Plasma-Deposited Coatings

The static contact angle of the coatings was measured using a goniometer (OneAttension Theta, Biolin Scientific, Vastra Frolunda, Sweden) connected to a video-camera system, according to the sessile drop method. First, a 5 µL droplet of Milli-Q water (Sigma Aldrich, Burlington, MA, USA) was drop-casted onto the sample surface, and then the static contact angle was read at 10 s. The evolution of the droplet volume was also monitored over the period of 300 s. The measurements were carried out in three replicates at four different locations on the sample, and the data are expressed as means ± standard deviations. FTIR spectroscopy (Vertex 70 (Bruker®, Billerica, MA, USA) in attenuated total reflectance (ATR) mode was used to analyze the chemical composition of the pristine substrate surface as well as the surface of the plasma-modified substrate before and after immersion in different FS solutions. To ensure good contact (typically a few microns in depth), the samples were pressed on a diamond crystal by a fixed force. Each spectrum (average of 52 scans) was recorded in the range of 500–4000 cm^{-1}, at a spectral resolution of 4 cm^{-1}, and the baseline was corrected by setting the minima in the 2500–1800, 3600–3000, and 3800–4000 cm^{-1} regions to zero. The morphology of the plasma-deposited organosilicon coatings was examined using a JSM7600F scanning electron microscope (SEM; JEOL, Saint-Hubert, QC, Canada) equipped with a field emission (FE) electron emitter. All images were recorded in secondary electron (SE) mode at an acceleration voltage of 5 kV. To prevent distortion and charging effects, the samples were coated with a 2-nm-thick layer of gold prior to SEM observation. After immersion in FS solutions, the chemical distribution of carbon (C) and silicon (Si) on the plasma-treated surfaces was analyzed using an energy-dispersive X-ray spectroscopy (EDS) system coupled to the SEM. The amount of silicon released from the organosilicon coating into DI water and heptane was determined using a Thermo Icap ICP-OES dual-view device (Thermo Fisher Scientific, Waltham, MA, USA) equipped with an alumina injector. The analytes were introduced into the device via a mini crossflow nebulizer and an Ultem spray chamber, and then they were digested with 47% hydrofluoric acid (HF). The volume was adjusted to 10 mL prior to each analysis.

2.4. Statistical Analysis

The contact angle and silicon release data reported herein are expressed as mean ± standard deviation, and they were statistically analyzed using the one-way ANOVA function in Origin Pro 2015 [60]. Comparisons with p-values less than 0.05 were considered to be significantly different.

3. Results and Discussion

3.1. Wettability and Absorption

In wet packaging applications, it is imperative that the materials used maintain their hydrophobic properties under different conditions. For instance, paper cups must be designed in such a way that they remain dry and intact when they meet liquids, including hot beverages. Therefore, the wettability of this packaging material must be tested

under both, high and low temperature conditions. Herein, the wettability and stability of organosilicon-coated Kraft paper were assessed by measuring the water contact angle of the samples before and after immersion in different FS solutions under varying conditions of immersion time, temperature, and shaking rate.

3.1.1. Effect of Time

Considering that disposable food packaging products may remain in contact with food articles for extended periods of time (up to 3–4 h), it is necessary that the plasma-treated cellulosic materials prepared in this study maintain their hydrophobic properties as long as possible. Figure 1 presents the variation of water contact angle (WCA) as a function of liquid exposure time for different Kraft paper samples. Notably, the untreated sample completely and rapidly absorbs the aqueous droplet (<200 ms), as it is hydrophilic, and thus, its static WCA cannot be determined. After plasma deposition, the cellulosic substrate surface becomes highly hydrophobic due to the presence of hydrophobic functional groups such as methyl and methylene in the PDMS-like plasma-polymer HMDSO (ppHMDSO) coating [61,62]. Indeed, the static WCA value of the ppHMDSO-coated sample is 132 $\pm$ 8°, which confirms that no oxidizing gaseous species are present during the fragmentation of organosilicon precursors in the plasma [63]. Considering the porous structure of Kraft paper, the plasma-generated species can easily diffuse into the pores of the substrate, thereby rendering the inner fibers hydrophobic as well [54,56].

Additionally, to assess the effects of different FS liquids on the hydrophobicity of plasma-treated Kraft paper, the wettability of this paper was measured after immersion and shaking in DI water, acetic acid solution, ethanol solution, and heptane at 40 °C for different time durations. The results obtained (Figure 1a) show that the ppHMDSO-coated paper samples maintain their hydrophobic nature even after 24 h of immersion and shaking, irrespective of the chemical nature of the FS. Indeed, the static WCA values determined after immersion are not significantly different from the values determined before ($p > 0.05$), and in fact, they are slightly higher. The WCAs of samples immersed in the same liquid medium for different periods of time (0.5, 3, 16, or 24 h) also exhibit variations, albeit insignificant ($p > 0.05$). These variations may be attributed to changes in the micro-/nano-roughness and chemical composition of the analyzed surface after interaction with the liquids. Coating removal and fiber swelling can also modify the macroscopic structure of the cellulosic network [56].

Although immersion-induced changes in the WCA of plasma-treated paper are observed, no obvious trend can be inferred, probably due to the complexity of the interactions between the ppHMDSO coating and the liquids as well as the relatively large deviation between the measured values. Such a large deviation may be attributed to the effect of shaking in changing the organization of fibers, which alters the macroroughness of the analyzed surface. According to previous studies, the penetration of liquids into polymer films is affected by many parameters, including film porosity, chemistry, and mechanical properties [63]. Several models available in the literature can be used to describe the diffusion of liquids in such systems; however, no unique model can simulate the highly system-specific and complicated mechanisms involved in the penetration process [64–66]. Apart from penetration, some liquids react with the deposited coating, which further complicates the diffusion process. For instance, the hydrolysis of ppHMDSO siloxane bonds in the presence of water results in the generation of hydrophilic Si-OH groups that promote the penetration of water molecules into the coating [67,68]. This shows that the plasma-deposited organosilicon coating prepared herein may undergo different penetration mechanisms in different FS solutions, resulting in variable morphological changes due to swelling.

At this stage, one must consider that different water absorption properties are required for different food packaging applications. For example, it is desired that tissues and towels take up water quickly, while paper cups and food containers must be water-resistant. Recently, great efforts have been made to fully understand the process of water

absorption and transport via modeling and experimental research [65,69,70]. However, the absorption behavior of water remains ambiguous due to the complex structure of fibrous substrates. To examine the effects of food simulants on the absorption behavior of the paper, measurements were also conducted after immersion and shaking in different FS solutions for different time durations. Figure 1b presents the values corresponding to the difference between static WCAs measured at 10 and 300 s. These values reflect the stability of the ppHMDSO coating after immersion in the FSs. Although significant variations between the ΔCA values of samples immersed in different liquids are observed ($p < 0.05$), no major temporal change in CA is detected (ΔCA < 3°) within 300 s, except in the case of plasma-treated samples immersed in heptane for 16 and 24 h. For these two samples, the difference in contact angles (CA_{10s}–CA_{300s}) drastically increases to almost 140°, probably due to coating removal after immersion in heptane, which is a good solvent for organosilicon species [64,66]. Moreover, the ΔCA values of samples immersed in DI water, ethanol, and acetic acid do not appreciably depend on the immersion time ($p > 0.05$); however, the values corresponding to samples immersed in heptane do ($p < 0.05$).

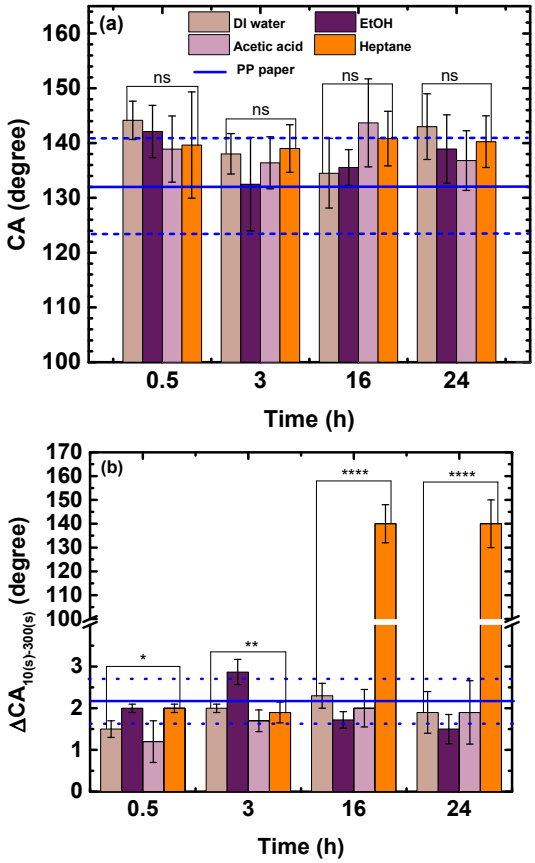

Figure 1. (**a**) Mean static WCA values of ppHMDSO-coated Kraft paper samples immersed in different FS solutions (DI water, ethanol, acetic acid, and heptane) at 40 °C for different periods of time, and (**b**) the difference between the static WCA values measured at 300 and 10 s. The solid and dashed blue lines represent the mean and max/min values obtained for non-immersed ppHMDSO-coated Kraft paper, respectively. ns: not significant, $p > 0.05$; * $p < 0.05$; ** $p < 0.01$; **** $p < 0.0001$.

The water uptake capacity and dynamic water absorption of plasma-treated Kraft paper were also assessed by monitoring the volume of 5 µL water droplets settled on the surface of each sample over a period of 300 s. For comparison, samples immersed in DI water and heptane were analyzed. As shown in Figure 2a, all droplets cast onto samples immersed in DI water exhibit a decreasing volume trend, irrespective of the immersion time; however, the rate of decrease varies significantly ($p < 0.05$), with the fastest and slowest rates observed for the 0.5 and 24 h immersion samples, respectively.

Notably, the time needed to completely absorb the droplet is greater than 300 s, which agrees well with our previous reports concerning the absorption time of plasma-deposited hydrophobic coatings on cellulosic substrates [54]. Considering that the volume profiles of non-immersed (blue line in Figure 2a) and water-immersed plasma-modified paper are similar, it may be concluded that the hydrophobic ppHMDSO coating is not affected by DI water and that the temporal variation in droplet volume is attributed to water evaporation rather than absorption by the surface or penetration through the coating. It must be noted that the rate of water evaporation may change from one day to the next due to variations in temperature and pressure. The temporal profiles presented in Figure 2b demonstrate that the ppHMDSO-coated paper samples immersed in heptane solution for 0.5 or 3 h exhibit only a 16% reduction in the volume of water droplets cast onto their surface. Such a small reduction in volume is most likely attributed to water evaporation, as explained above. Meanwhile, the samples immersed in heptane for 16 and 24 h exhibit full absorption of the water droplet at 160 and 90 s, respectively. These results are consistent with the water uptake data (Figure 1b), and they suggest that prolonged exposure of the plasma-modified Kraft paper to heptane leads to coating removal due to the solubility of this silicon-based coating in hydrocarbon solvents [64,66].

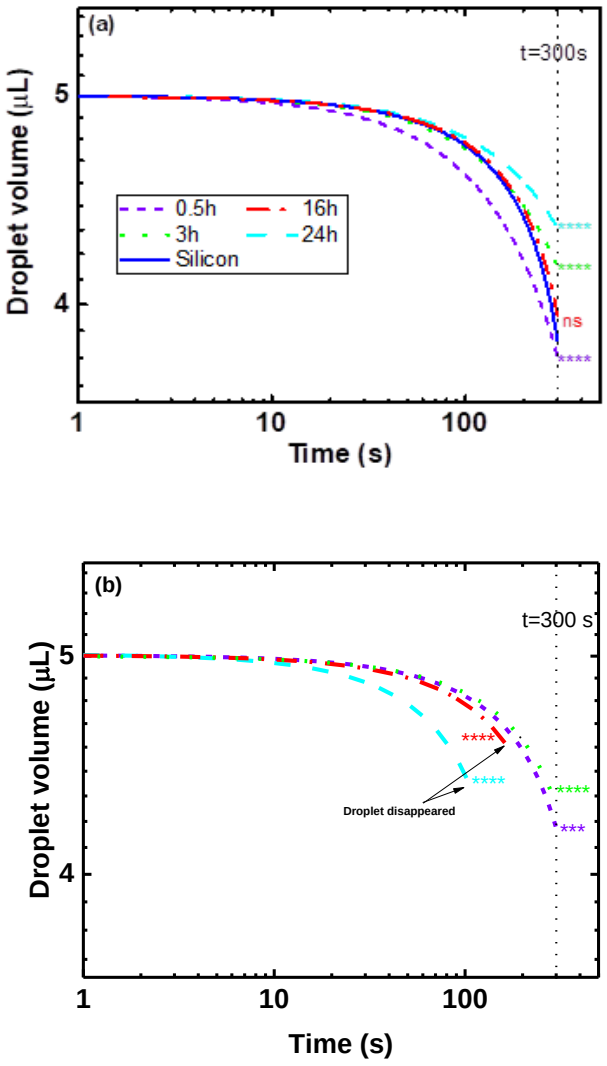

Figure 2. Temporal variation in the volume of a 5 µL water droplet deposited onto the surface of plasma-modified paper samples immersed in (**a**) DI water and (**b**) heptane for different periods of time. The volume profile of the water droplet cast onto non-immersed paper is also shown for comparison (blue line). ns: not significant, $p > 0.05$; *** $p < 0.001$; **** $p < 0.0001$ vs. silicon.

3.1.2. Effects of Stirring Rate and Temperature

The HPFB recommends that migration experiments be run under the most severe conditions. Therefore, the effects of extreme temperatures and stirring rates on the hydrophobicity of ppHMDSO-coated paper samples immersed in different FS solutions were also examined. Considering that immersion time does not significantly affect the absorption behavior of the paper, as detailed in Section 3.1.1, all samples were analyzed after 3 h of immersion. Figure 3a depicts the effect of stirring rate on the static WCA of samples immersed in DI water, ethanol solution, acetic acid solution, and heptane at 65 °C, and it shows that in the range of 50–140 rpm, the hydrophobic properties of these samples remain intact. This is evidenced by the similar static WCA values measured at 50 and 140 rpm ($p > 0.05$). The stability of the samples is also preserved under different stirring rates, as confirmed by the $\Delta CA_{10(s)-300(s)}$ data presented in Figure 3b. Therefore, it may be concluded that within the range of experimental conditions investigated herein, the stirring rate has no substantial effect on the plasma-deposited coating, which remains firmly attached to the substrate.

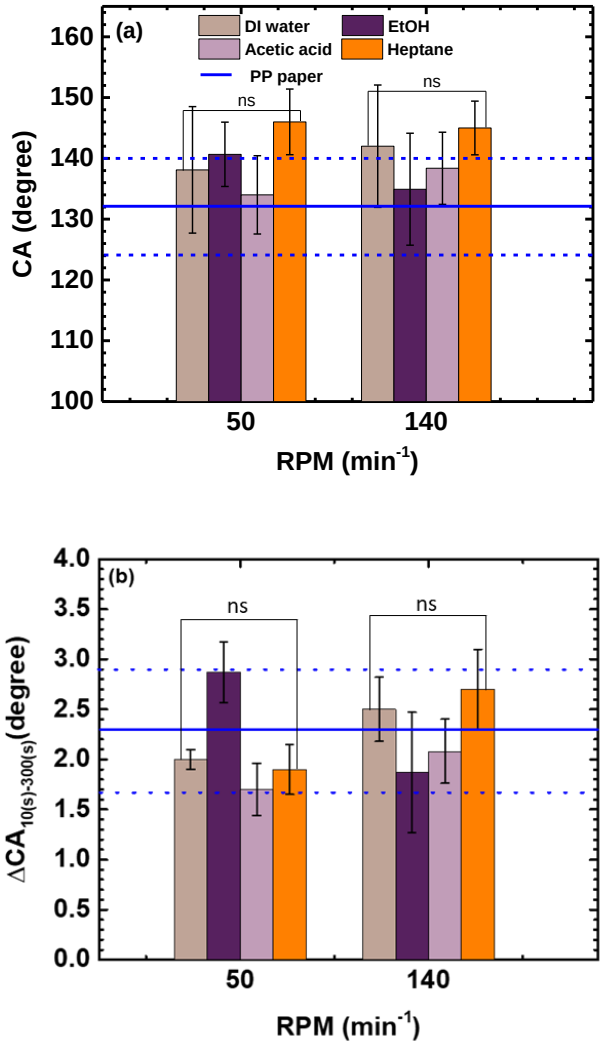

Figure 3. Influence of shaking rate on the (**a**) static WCA values and (**b**) $\Delta CA_{10(s)-300(s)}$ values of plasma-modified paper samples immersed in different FS solutions for 3 h at 65 °C. The solid and dashed blue lines represent the mean and max/min values obtained for non-immersed ppHMDSO-coated Kraft paper, respectively. ns: not significant, $p > 0.05$.

The results illustrated in Figure 4a,b demonstrate that similar to the stirring rate, the temperature has no significant effect on the hydrophobicity and stability of the investigated

samples, respectively, as the static WCA and $\Delta CA_{10(s)-300(s)}$ values measured at different temperatures in the range of 23–65 °C are not significantly different ($p > 0.05$). Interestingly, the samples immersed in heptane exhibit the greatest variation in static WCA (smallest p-value), while those immersed in ethanol exhibit the least variation (largest p-value). However, no obvious trend may be discerned. Overall, the static WCA values, water uptake, and water absorption results obtained herein indicate that the ppHMDSO coating deposited by atmospheric-pressure plasma onto Kraft paper substrates is highly hydrophobic. The hydrophobicity and stability of this coating are maintained after prolonged immersion in food simulant solutions, even under harsh temperature and stirring rate conditions, except in the case of heptane. The samples immersed and shaken in a non-polar heptane solvent for 16 or more hours lose their ppHMDSO coating and thus no longer have a hydrophobic surface.

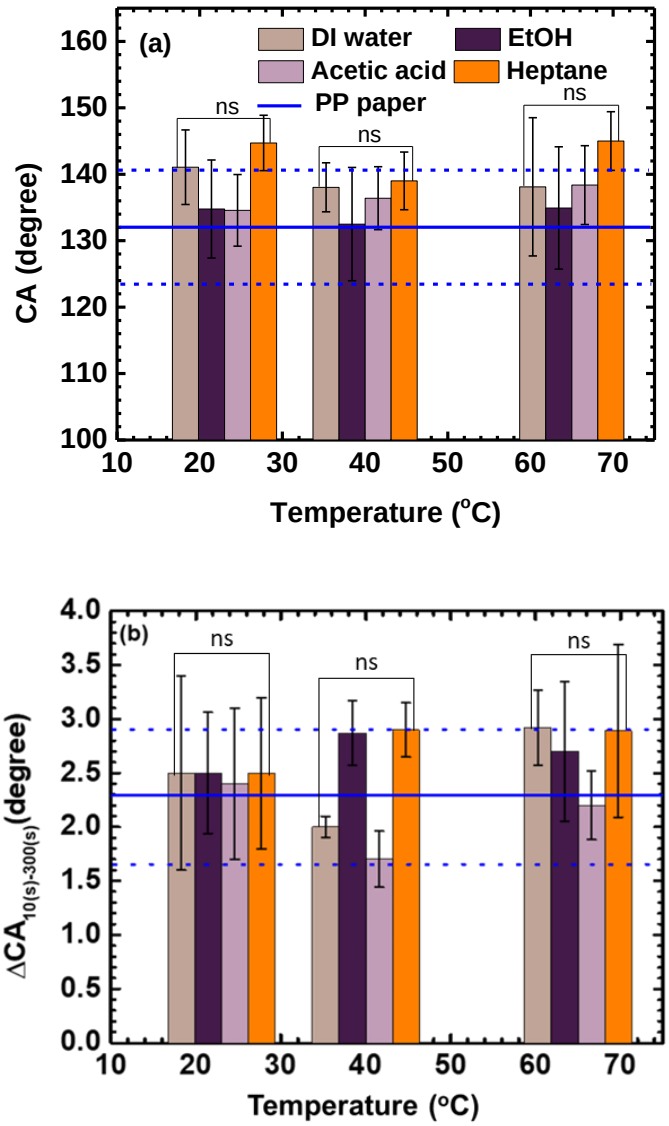

Figure 4. Influence of temperature on the (**a**) static WCA values and (**b**) $\Delta CA_{10(s)-300(s)}$ values of plasma-modified paper samples immersed in different FS solutions for 3 h at 50 rpm. The solid and dashed blue lines represent the mean and max/min values obtained for non-immersed ppHMFDSO-coated Kraft paper, respectively. ns: not significant, $p > 0.05$.

3.2. Chemical Composition

The chemical modifications of plasma-treated sample surfaces induced by interaction with different liquids were analyzed by ATR-FTIR spectroscopy. The spectra recorded

before (blue) and after immersion in DI water (marron), acetic acid (light purple), ethanol (dark purple), and heptane (orange) at 40 °C for 3 h are shown in Figure 5. The signals detected in the spectrum of as-deposited paper (i.e., before immersion) are similar to those observed for typical PDMS-like structures [67], and they have been comprehensively identified in previous studies [54–56]. Briefly, the intense band between 1150 and 950 cm^{-1} is assigned to the SiOSi and SiOC asymmetric stretching modes [68]. This band is considered to be the sum of three Gaussian components at 1100, 1070, and 1020 cm^{-1}, corresponding to different vibrational modes in conformations with 170–180, 140, and 120° SiOSi bond angles, respectively [67,68,71]. The first component corresponds to SiOSi stretching; the second corresponds to in-phase asymmetric stretching of neighboring OSiO moieties; and the third is related to the methyl environment of SiOSi. Two strong, sharp peaks ascribed to the asymmetric and symmetric bending of the CH_3 group in $SiCH_3$ are also detected at 1256 cm^{-1}. The peak at 847 cm^{-1} is attributed to Si-C rocking, whereas the band at 800 cm^{-1} comprises two peaks (800 and 760 cm^{-1}) that are ascribed to CH_3 rocking in $Si(CH_3)_3$ and $Si(CH_3)_2$. The positions of these peaks may be shifted to higher wavenumbers depending on the oxidation degree of the surrounding Si atoms [18]. As for the band between 3000 and 2900 cm^{-1}, it is classically assigned to CH_3 asymmetric and symmetric stretching. Although the chemical signature of the cellulose substrate is visible between 500 and 1500 cm^{-1}, the spectrum of the as-deposited sample does not show any absorption of cellulosic OH in the region between 3600 and 3000 cm^{-1} [54–56], probably due to the relatively large thickness of the organosilicon layer, which impedes the detection of substrate functional groups.

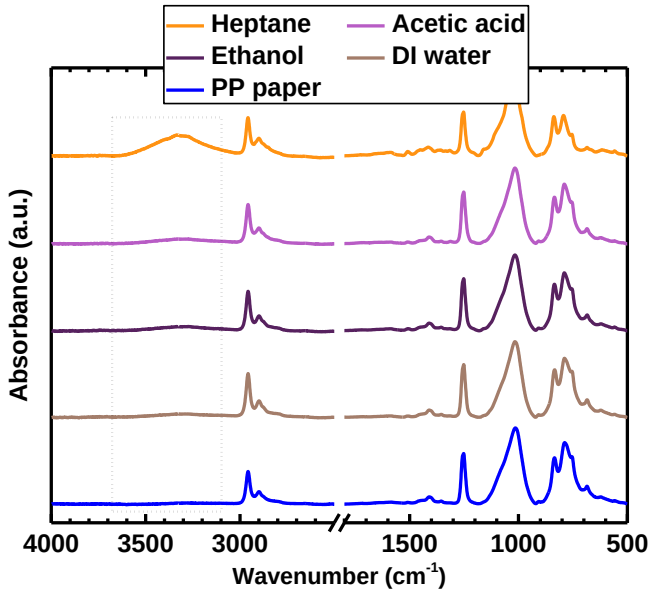

Figure 5. ATR-FTIR spectra of ppHMDSO-coated samples before and after immersion in different FS solutions for 3 h at 40 °C (after baseline correction).

Considering that the ATR-FTIR spectra of the samples immersed in DI water, ethanol, and acetic acid are similar to the as-deposited substrate spectrum, these food simulants do not affect the composition of the plasma-deposited organosilicon film within the range of conditions investigated herein. However, the chemical signature of the plasma-treated sample changes after immersion in heptane. Specifically, the OH band attributed to cellulose appears in the spectrum after immersion, which highlights the effect of the heptane hydrocarbon solvent in dissolving the organosilicon coating and exposing the OH groups in cellulose. Moreover, a slight decrease in the intensities of the 760 and 795 cm^{-1} absorption peaks corresponding to CH_3 rocking in $Si(CH_3)_2$ and $Si(CH_3)_3$ is observed, which suggests that the thickness of the organosilicon layer is reduced upon immersion and shaking in

heptane for 3 h (40 °C). Based on the theoretical depth of light penetration, the thickness of the layer after immersion is estimated at 0.5 µm.

According to previous works [54–56], the ratio of the OH band area at 3600–3000 cm^{-1} to the SiOSi stretching vibration band area at 1020 cm^{-1} is inversely proportional to the thickness of the deposited film, as illustrated in Equation (1):

$$Thickness\ ratio(OH) = \frac{\int\ OH(3200\ cm^{-1})}{\int\ SiOSi\ (1020\ cm^{-1})} \quad (1)$$

In order to evaluate the evolution of the ppHMDSO layer thickness under different conditions, the thickness ratio (R) was calculated for each sample. Compared to the as-deposited substrate (R = 0.03), the R values of the samples immersed in DI water, ethanol, and acetic acid increase slightly (R = 0.06, 0.12, and 0.11, respectively), which indicates that these solutions slightly alter the thickness of the ppHMDSO film. Considering that DI water, ethanol, and acetic acid have no appreciable effect on the chemical composition of the plasma-deposited coating, it may be concluded that the slight change in static WCA value detected after immersion in these solutions is attributed to the modification of macro- and micro-roughness rather than the alteration of chemical composition. In the case of heptane, the R value increases significantly after immersion (R = 0.32), which confirms that this solvent partially dissolves the plasma-deposited organosilicon layer on cellulose. These results are in good agreement with the dynamic WCA data discussed above.

In theory, the wettability of a surface depends on its roughness and chemical composition. A change in either one of these two parameters may lead to variations in WCA angles. Based on the ATR-FTIR data discussed above, heptane dissolves the ppHDMSO coating on cellulose substrates, thereby exposing the cellulosic OH groups and altering the chemical composition of the sample surface. The change in surface chemical composition explains the important variation in WCA observed upon immersion of the ppHMDSO-coated samples in heptane. In the case of samples immersed in DI water, ethanol, or acetic acid, the chemical composition of the surface is not significantly changed. Therefore, changes in the WCA values of these samples (before and after immersion) may not be attributed to variations in surface chemical compositions, at least those observed over the micrometer scale probed by ATR-FTIR analyses. Instead, these changes may be induced by other parameters affecting the penetration of liquids into polymer films, such as film porosity and mechanical properties [18]. Different models available in the literature may be used to assess the effects of these parameters and describe the diffusion behavior of liquids. However, no unique model can accurately portray the penetration phenomenon in our system due to the complexity and specificity of the implicated mechanisms [72–74]. Chemical interactions between the plasma-deposited coating and the liquids further complicate the diffusion process. For instance, the hydrophilic Si-OH groups produced upon the hydrolysis of ppHMDSO films in water promote the penetration of water molecules into the films, thereby inducing swelling and roughness modification [75,76]. In this regard, each FS solution tested herein may experience penetration mechanisms different from the other solutions.

3.3. Morphology

Pristine paper substrates are characterized by a heterogeneous fiber web structure with a given porosity and surface roughness. Considering that this structure may be altered by food simulants, morphological analyses were conducted before and after immersion of the ppHMDSO-coated cellulose substrate in FS solutions. The SEM image presented in Figure 6a shows that the as-deposited sample exposed to atmospheric-pressure HMDSO-based plasma for 30 min exhibits a lumpy, globular surface morphology with microfibers. Similar macrostructures on the surface of porous membranes with organosilicon coatings have been reported in other studies [55,77,78]. Since only heptane induces changes in the static WCA of the ppHMDSO coating, the morphology of the sample immersed in heptane for 24 h was analyzed, and it was compared to the morphology of the sample

immersed in DI water. As shown in Figure 6b, the original cauliflower-like microstructure of the organosilicon coating remains intact after immersion in DI water for 24 h; however, some cracks appear on the surface. During plasma deposition, certain regions on the substrate may remain uncovered by plasma-formed fragments. These regions constitute hydrophilic defects that facilitate the penetration of liquids into the substrate, resulting in fiber swelling. The stress induced by swollen fibers leads to the cracking of the layer. Notably, the cracks observed on the surface of plasma-modified samples immersed in DI water are relatively small, and thus, they do not have a strong impact on the static WCA and water absorption properties. Different from DI water, heptane significantly alters the morphology of ppHMDSO-coated cellulose, resulting in a smoother surface, as shown in Figure 6c. Moreover, certain regions on the sample surface are not covered by the ppHMDSO layer, probably due to the dissolution of the coating in heptane. Considering that the size of uncovered regions is comparable to that of substrate fibers (same order of magnitude), the absence of a coating in these regions may also be attributed to the separation of weakly attached fibers from the substrate during immersion and shaking. As explained above, non-coated regions on the sample surface are hydrophilic, and as such, they facilitate liquid penetration and fiber swelling, which in turn increases the static WCA value and micro-roughness of the sample. EDX mapping of plasma-modified Kraft paper samples immersed in DI water or heptane for 24 h shows that while the organosilicon coating remains intact after immersion in DI water (Figure 6d), small parts of it are lost after immersion in heptane (Figure 6e). In the latter case, the silicon signal is lost and only carbon is seen.

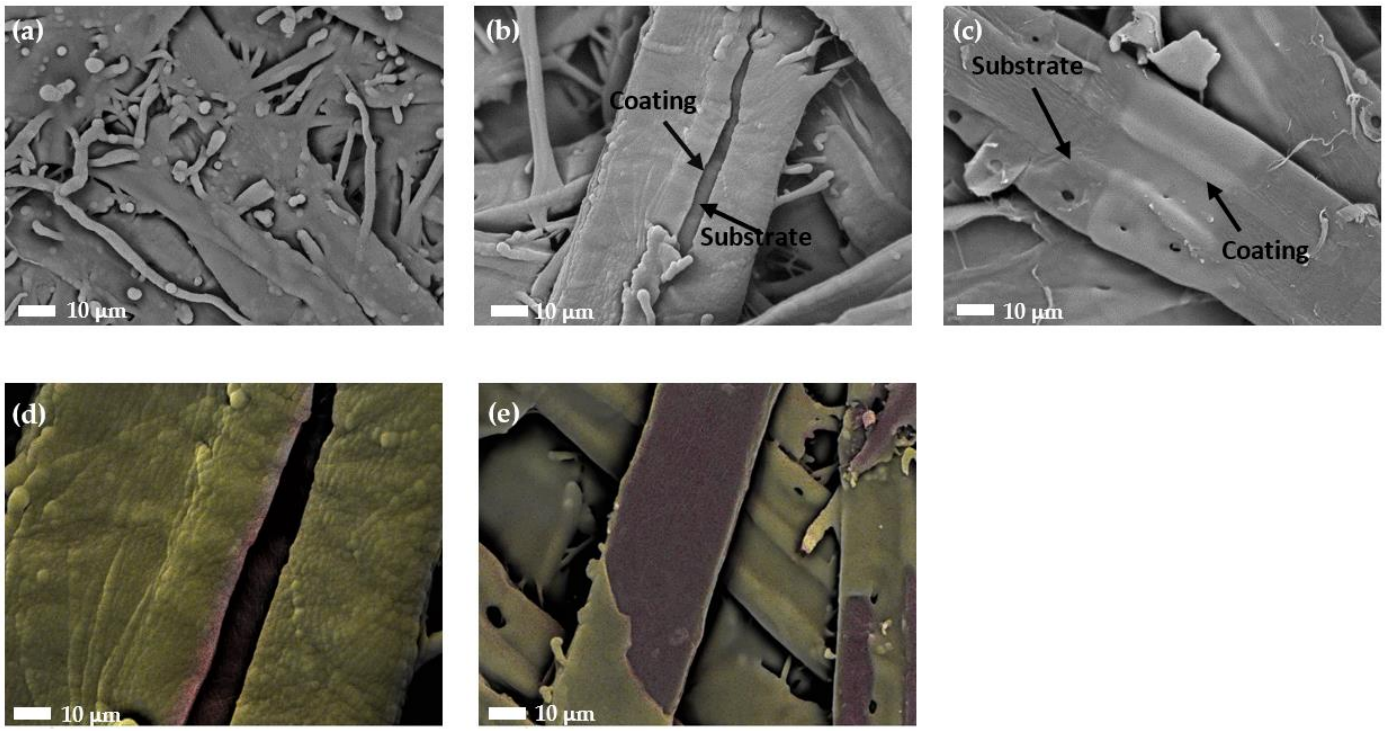

Figure 6. SEM images of plasma-modified Kraft paper surfaces recorded (**a**) before and after immersion in (**b**) DI water and (**c**) heptane at 40 °C for 24 h. EDX images of the sample surfaces after immersion in (**d**) DI water and (**e**) heptane. The olive and burgundy colors represent Si and C atoms, respectively.

3.4. Release of Silicon

During the last decade, there has been growing concern regarding the migration of low-molecular-weight compounds from food packaging materials to the contents. The available research is mostly focused on the migration of vinyl chloride monomers (VCM)

and plasticizers in polyvinyl chloride (PVC) packaging materials [41,43,44,50,51]. Herein, ICP-OES is used to assess the migration of silicon from plasma-modified Kraft paper to water or heptane under different temperatures and shaking rate conditions. As shown in Figure 7, the amount of silicon released into heptane is approximately ten times greater than that released into DI water, irrespective of the immersion time and condition. This is probably due to the effect of heptane in dissolving organosilicon species [64,66]. Although the Si amount released from samples immersed in heptane does not significantly depend on temperature ($p > 0.05$), the samples immersed in DI water clearly exhibit increased release at higher temperatures ($p < 0.05$) (Figure 7a). This agrees well with previous studies showing that the migration of volatile and nonvolatile chemicals from polypropylene (PP) or polyethylene terephalate (PET) to food is accelerated at elevated temperatures (~200 °C) [79]. Nevertheless, the temperature range investigated in this study is relatively narrow (25–65 °C), and more data points are needed to establish a trend. The effect of immersion time on migration is similar to that of temperature, with greater migration observed at longer times between 0 and 24 h (Figure 7b). However, the variation in the amount of silicon released at different times is not significant ($p > 0.05$), and thus, no clear trend can be established. In addition to temperature and immersion time, the effect of shaking rate on silicon migration was also examined. The obtained results demonstrate that higher shaking rates accelerate the release of silicon into DI water and heptane. However, significant acceleration is observed for samples immersed in DI water ($p < 0.05$), but not for those immersed in heptane ($p > 0.05$).

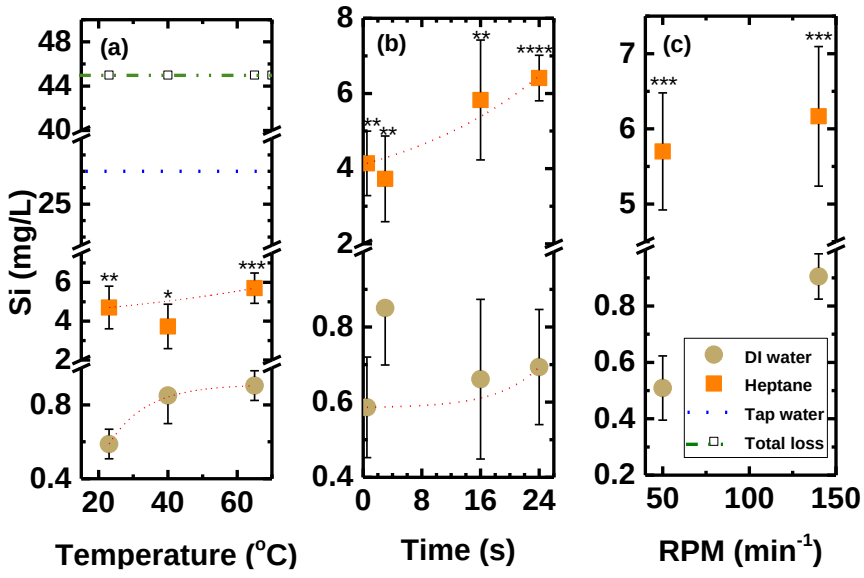

Figure 7. The amount of silicon released for the ppHMDSO coating into DI water and heptane at varying (**a**) temperatures (3 h immersion), (**b**) immersion times (40 °C), and (**c**) shaking rates (40 °C for 3 h). * $p < 0.05$; ** $p < 0.01$; *** $p < 0.001$; **** $p < 0.0001$.

Although the amount of silicon released into heptane is greater than that released into DI water, both quantities are less than the amount typically detected in tap water (5–25 mg/L [80]). To determine the fraction of silicon released into liquids, the total amount of silicon available in the coating was estimated. Considering that ppHMDSO is a PDMS-like polymer ($(C_2H_6SiO)_n$), as established in a previous study [18], its density was assumed to be equal to the PDMS density (0.97 gr/cm^3), and it was used to calculate the mass of ppHMDSO based on the coating dimensions. The surface area of the coating may be easily obtained; however, its thickness cannot be readily determined due to the porous nature of the substrate. Herein, it was considered that the thickness of the ppHMDSO film deposited on porous cellulose is equivalent to that of the coating deposited on a silicon substrate under the same conditions. This latter was found to be 200 nm. Although this value was

used to estimate the mass of the ppHMDSO from density, it must be noted that the true thickness of the coating deposited on Kraft paper is actually less than 200 nm due to the penetration of plasma species through the pores of cellulosic substrates [54–56]. Based on the estimated density and coating dimensions (1.2 cm × 2.1 cm × 200 nm), the total mass of the plasma-deposited coating is 0.048 mg. Considering that the mass of a single PDMS molecule is 12.29×10^{-23} g, the repetition factor of the polymer in the coating is 4×10^{17}, which corresponds to ~0.018 mg of silicon. If all of this silicon were to be released into the FS immersion solution (4 mL), the concentration of Si in the solution would be 45 mg/L. On average, the Si concentrations detected experimentally in DI water and heptane are <0.9 and ~5.4 mg/L, respectively. Therefore, it may be concluded that the ppHMDSO coating loses less than 2% of its silicon in DI water, compared to 12% in heptane. Since the cellulose substrate is coated with ppHMDSO on one side only, part of the silicon detected in the solutions after paper immersion may be derived from the paper itself. To account for this part, the amount of silicon released from paper into DI water and heptane was measured by ICP-OES. In both cases, the amount of Si released into the solution was found to be negligible (~0.04 ± 0.01 mg/L). This demonstrates that silicon does not migrate from paper or paperboard packaging materials [81–83].

4. Conclusions

Kraft paper was successfully modified using an environmentally friendly plasma approach. An atmospheric pressure dielectric barrier discharge ignited in a He/HMDSO atmosphere was used to deposit an organosilicon-based hydrophobic layer on the surface of FC films. ATR-FTIR analyses show that organic species such as SiC and $SiCH_3$ are present on the surface of plasma-modified substrates, which indicates that the deposited coating is hydrophobic. Wettability measurements further confirm the hydrophobicity of the coating, whose static water contact angle is 132 ± 8°. To validate the applicability of plasma-deposited organosilicon coatings in the food and packaging industries, the effects of different food simulants such as DI water, 95% ethanol, 5% acetic acid, and heptane on the morphology, chemical composition, and wettability of plasma-modified FC films were investigated under various conditions of temperature, immersion time, and shaking rate. The results obtained show that among the tested FS solutions, only heptane has a significant impact on the coating thickness. Furthermore, the WCA of the coating is not altered upon immersion in FS solution, and the sample surface remains hydrophobic regardless of the shaking and immersion conditions. However, prolonged immersion (>16 h) in heptane leads to reduced water absorbency due to the dissolution of the organosilicon coating, as evidenced by morphological analysis. The low rate of silicon release measured herein further confirms that the hydrophobic nature of the plasma-deposited organosilicon coating is not compromised by contact with different food simulants. Therefore, this coating has great potential for use in wet packaging applications. In general, this study provides a green alternative for the preparation of paper products with hydrophobic properties.

Author Contributions: Conceptualization, J.P., A.D., S.A., A.S. and L.S.; formal analysis, S.B.; funding acquisition, L.S.; investigation, J.P. and S.B.; methodology, J.P. and L.S.; project administration, L.S.; supervision, L.S.; validation, S.B. and M.A.R.; writing—original draft, S.B.; writing—review and editing, J.P., M.A.R., A.D., S.A., A.S. and L.S. All authors have read and agreed to the published version of the manuscript.

Funding: This work was financially supported by the National Science and Engineering Research Council (NSERC), PRIMA-Québec, Plasmionique Inc., and FPInnovations.

Institutional Review Board Statement: Not applicable.

Informed Consent Statement: Not applicable.

Data Availability Statement: The datasets generated and analyzed in this study are available from the corresponding author upon reasonable request.

Conflicts of Interest: The authors declare no conflict of interest.

References

1. Ciolacu, D.; Popa, V.I. Cellulose allomorphs: Structure, accessibility and reactivity. *Environ. Eng. Manag. J.* **2011**, *10*, 467–468.
2. Gadhave, R.V.; Gadhave, C.R.; Dhawale, P.V. Plastic-free bioactive paper coatings, way to next-generation sustainable paper packaging application: A review. *Green Sustain. Chem.* **2022**, *12*, 9–27. [CrossRef]
3. Dey, A.; Sengupta, P.; Pramanik, N.K.; Alam, T. Paper and other pulp based eco-friendly moulded materials for food packaging applications: A review. *J. Postharvest Technol.* **2020**, *8*, 01–21.
4. Wang, Q.; Sun, J.; Yao, Q.; Ji, C.; Liu, J.; Zhu, Q. 3D printing with cellulose materials. *Cellulose* **2018**, *25*, 4275–4301. [CrossRef]
5. Gao, B.; Li, X.; Yang, Y.; Chu, J.; He, B. Emerging paper microfluidic devices. *Analyst* **2019**, *144*, 6497–6511. [CrossRef] [PubMed]
6. Andresen, M.; Johansson, L.-S.; Tanem, B.S.; Stenius, P. Properties and characterization of hydrophobized microfibrillated cellulose. *Cellulose* **2006**, *13*, 665–677. [CrossRef]
7. Garcia-Ubasart, J.; Colom, J.F.; Vila, C.; Gomez Hernandez, N.; Blanca Roncero, M.; Vidal, T. A new procedure for the hydrophobization of cellulose fibre using laccase and a hydrophobic phenolic compound. *Bioresour. Technol.* **2012**, *112*, 341–344. [CrossRef]
8. Forsman, N.; Lozhechnikova, A.; Khakalo, A.; Johansson, L.S.; Vartiainen, J.; Osterberg, M. Layer-by-layer assembled hydrophobic coatings for cellulose nanofibril films and textiles, made of polylysine and natural wax particles. *Carbohydr. Polym.* **2017**, *173*, 392–402. [CrossRef]
9. Levasseur, O.; Vlad, M.; Profili, J.; Gherardi, N.; Sarkissian, A.; Stafford, L. Deposition of fluorocarbon groups on wood surfaces using the jet of an atmospheric-pressure dielectric barrier discharge. *Wood Sci. Technol.* **2017**, *51*, 1339–1352. [CrossRef]
10. Rodionova, G.; Lenes, M.; Eriksen, Ø.; Gregersen, Ø. Surface chemical modification of microfibrillated cellulose: Improvement of barrier properties for packaging applications. *Cellulose* **2010**, *18*, 127–134. [CrossRef]
11. Xu, Y.; Chen, Y.; Zhao, Z.; Xu, S. Process variables and the performance of soybean-oil rosin-based polyester as an internal sizing agent. *BioResources* **2019**, *14*, 9183–9197. [CrossRef]
12. Goncalves, G.; Marques, P.A.; Trindade, T.; Neto, C.P.; Gandini, A. Superhydrophobic cellulose nanocomposites. *J. Colloid Interface Sci.* **2008**, *324*, 42–46. [CrossRef] [PubMed]
13. Roy, D.; Guthrie, J.T.; Perrier, S. graft polymerization: Grafting poly(styrene) from cellulose via reversible addition-fragmentation chain transfer (RAFT) polymerization. *Macromolecules* **2005**, *38*, 10363–10372. [CrossRef]
14. Takács, E.; Wojnárovits, L.; Borsa, J.; Rácz, I. Hydrophilic/hydrophobic character of grafted cellulose. *Radiat. Phys. Chem.* **2010**, *79*, 467–470. [CrossRef]
15. Morandi, G.; Heath, L.; Thielemans, W. Cellulose nanocrystals grafted with polystyrene chains through surface-initiated atom transfer radical polymerization (SI-ATRP). *Langmuir* **2009**, *25*, 8280–8286. [CrossRef]
16. Avramidis, G.; Hauswald, E.; Lyapin, A.; Militz, H.; Viöl, W.; Wolkenhauer, A. Plasma treatment of wood and wood-based materials to generate hydrophilic or hydrophobic surface characteristics. *Wood Mater. Sci. Eng.* **2009**, *4*, 52–60. [CrossRef]
17. Bente, M.; Avramidis, G.; Förster, S.; Rohwer, E.G.; Viöl, W. Wood surface modification in dielectric barrier discharges at atmospheric pressure for creating water repellent characteristics. *Holz Als Roh Werkst.* **2004**, *62*, 157–163. [CrossRef]
18. Blanchard, N.E.; Naik, V.V.; Geue, T.; Kahle, O.; Hegemann, D.; Heuberger, M. Response of plasma-polymerized hexamethyldisiloxane films to aqueous environments. *Langmuir* **2015**, *31*, 12944–12953. [CrossRef]
19. Cunha, A.G.; Freire, C.S.R.; Silvestre, A.J.D.; Neto, C.P.; Gandini, A.; Orblin, E.; Fardim, P. Highly hydrophobic biopolymers prepared by the surface pentafluorobenzoylation of cellulose substrates. *Biomacromolecules* **2007**, *8*, 1347–1352. [CrossRef]
20. Deslandes, Y.; Pleizier, G.; Poire, E.; Sapieha, S.; Wertheimer, M.R.; Sacher, E. The surface modification of pure cellulose paper induced by low-pressure nitrogen plasma treatment. *Plasmas Polym.* **1998**, *3*, 61–76. [CrossRef]
21. Foroughi Mobarakeh, L.; Jafari, R.; Farzaneh, M. Superhydrophobic Surface Elaboration Using Plasma Polymerization of Hexamethyldisiloxane (HMDSO). *Adv. Mater. Res.* **2011**, *409*, 783–787. [CrossRef]
22. Levasseur, O.; Stafford, L.; Gherardi, N.; Naudé, N.; Blanchard, V.; Blanchet, P.; Riedl, B.; Sarkissian, A. Deposition of hydrophobic functional groups on wood surfaces using atmospheric-pressure dielectric barrier discharge in helium-hexamethyldisiloxane gas mixtures. *Plasma Process. Polym.* **2012**, *9*, 1168–1175. [CrossRef]
23. Nithya, E.; Radhai, R.; Rajendran, R.; Shalini, S.; Rajendran, V.; Jayakumar, S. Synergetic effect of DC air plasma and cellulase enzyme treatment on the hydrophilicity of cotton fabric. *Carbohydr. Polym.* **2011**, *83*, 1652–1658. [CrossRef]
24. Nouicer, I.; Sahli, S.; Kihel, M.; Ziari, Z.; Bellel, A.; Raynaud, P. Superhydrophobic surface produced on polyimide and silicon by plasma enhanced chemical vapour deposition from hexamethyldisiloxane precursor. *Int. J. Nanotechnol.* **2015**, *12*, 597–607. [CrossRef]
25. Odrášková, M.; Szalay, Z.; Ráheľ, J.; Zahoranová, A.; Černák, M. Diffuse coplanar surface barrier discharge assisted deposition of water repellent films from N2/HMDSO mixtures on wood surface. In Proceedings of the 28th ICPIG, Prague, Czech Republic, 15–20 July 2007.
26. Enache, I.; Caquineau, H.; Gherardi, N.; Paulmier, T.; Maechler, L.; Massines, F. Transport phenomena in an atmospheric-pressure Townsend discharge fed by N2/N2O/HMDSO mixtures. *Plasma Process. Polym.* **2007**, *4*, 806–814. [CrossRef]
27. Levasseur, O.; Stafford, L.; Gherardi, N.; Naudé, N.; Beche, E.; Esvan, J.; Blanchet, P.; Riedl, B.; Sarkissian, A. Role of substrate outgassing on the formation dynamics of either hydrophilic or hydrophobic wood surfaces in atmospheric-pressure, organosilicon plasmas. *Surf. Coat. Technol.* **2013**, *234*, 42–47. [CrossRef]
28. Hsieh, C.-T.; Chang, B.-S.; Lin, J.-Y. Improvement of water and oil repellency on wood substrates by using fluorinated silica nanocoating. *Appl. Surf. Sci.* **2011**, *257*, 7997–8002. [CrossRef]

29. Mai, C.; Militz, H. Modification of wood with silicon compounds. Treatment systems based on organic silicon compounds–a review. *Wood Sci. Technol.* **2004**, *37*, 453–461. [CrossRef]
30. Podgorski, L.; Bousta, C.; Schambourg, F.; Maguin, J.; Chevet, B. Surface modification of wood by plasma polymerisation. *Pigment Resin Technol.* **2001**, *31*, 33–40. [CrossRef]
31. Potočňáková, L.; Hnilica, J.; Kudrle, V. Increase of wettability of soft- and hardwoods using microwave plasma. *Int. J. Adhes. Adhes.* **2013**, *45*, 125–131. [CrossRef]
32. Riedl, B.; Angel, C.; Prégent, J.; Blanchet, P.; Stafford, L. Effect of wood surface modification by atmospheric-pressure plasma on waterborne coating adhesion. *BioResources* **2014**, *9*, 4908–4923. [CrossRef]
33. Sèbe, G.; Brook, M.A. Hydrophobization of wood surfaces: Covalent grafting of silicone polymers. *Wood Sci. Technol.* **2001**, *35*, 269–282. [CrossRef]
34. Rehn, P.; Wolkenhauer, A.; Bente, M.; Förster, S.; Viöl, W. Wood surface modification in dielectric barrier discharges at atmospheric pressure. *Surf. Coat. Technol.* **2003**, *174–175*, 515–518. [CrossRef]
35. Vander Wielen, L.C.; Östenson, M.; Gatenholm, P.; Ragauskas, A.J. Surface modification of cellulosic fibers using dielectric-barrier discharge. *Carbohydr. Polym.* **2006**, *65*, 179–184. [CrossRef]
36. Lau, O.; Wong, S. Contamination in food from packaging material. *J. Chromatogr. A* **2000**, *882*, 255–270. [CrossRef]
37. Restuccia, D.; Spizzirri, U.G.; Parisi, O.I.; Cirillo, G.; Curcio, M.; Iemma, F.; Puoci, F.; Vinci, G.; Picci, N. New EU regulation aspects and global market of active and intelligent packaging for food industry applications. *Food Control* **2010**, *21*, 1425–1435. [CrossRef]
38. Bhunia, K.; Sablani, S.S.; Tang, J.; Rasco, B. Migration of chemical compounds from packaging polymers during microwave, conventional heat treatment, and storage. *Compr. Rev. Food Sci. Food Saf.* **2013**, *12*, 523–545. [CrossRef]
39. Reid, R.C.; Sldman, K.R.; Schwope, A.D.; Till, D.E. Loss of adjuvants from polymer films to foods or food simulants. effect of the external phase. *Ind. Eng. Chem. Prod. Res. Dev.* **1980**, *19*, 580–587. [CrossRef]
40. Kathuria, A.; Zhang, S. Sustainable and repulpable barrier coatings for fiber-based materials for food packaging: A review. *Front. Mater.* **2022**, *9*, 110556. [CrossRef]
41. Al Salloum, H.; Saunier, J.; Tfayli, A.; Yagoubi, N. Studying DEHP migration in plasticized PVC used for blood bags by coupling Raman confocal microscopy to UV spectroscopy. *Mater. Sci. Eng. C Mater. Biol. Appl.* **2016**, *61*, 56–62. [CrossRef]
42. Fankhauser-Noti, A.; Biedermann-Brem, S.; Grob, K. PVC plasticizers/additives migrating from the gaskets of metal closures into oily food: Swiss market survey June 2005. *Eur. Food Res. Technol.* **2006**, *223*, 447–453. [CrossRef]
43. Kawamura, Y.; Ogawa, Y.; Mutsuga, M. Migration of nonylphenol and plasticizers from polyvinyl chloride stretch film into food simulants, rapeseed oil, and foods. *Food Sci. Nutr.* **2017**, *5*, 390–398. [CrossRef]
44. Sero, R.; Nunez, O.; Javier Santos, F.; Moyano, E. Analytical methods for the determination of plasticizers in food and beverages. *Curr. Anal. Chem.* **2018**, *14*, 306–324. [CrossRef]
45. Zygoura, P.D.; Goulas, A.E.; Riganakos, K.A.; Kontominas, M.G. Migration of di-(2-ethylhexyl)adipate and acetyltributyl citrate plasticizers from food-grade PVC film into isooctane: Effect of gamma radiation. *J. Food Eng.* **2007**, *78*, 870–877. [CrossRef]
46. de Freitas, A.S.M.; Maciel, C.C.; Rodrigues, J.S.; Ribeiro, R.P.; Delgado-Silva, A.O.; Rangel, E.C. Organosilicon films deposited in low-pressure plasma from hexamethyldisiloxane—A review. *Vacuum* **2021**, *194*. [CrossRef]
47. Coclite, A.M.; Gleason, K.K. Initiated PECVD of organosilicon coatings: A new strategy to enhance monomer structure retention. *Plasma Processes Polym.* **2012**, *9*, 425–434. [CrossRef]
48. Salamianski, A.E.; Agabekov, V.E.; Chishankov, I.G.; Matveenko, Y.V.; Melnikova, G.B.; Nguyen, T.D.; Vu, K.O.; Pham, G.V.; Trinh, A.T.; Tran, D.L.; et al. Tribological and anticorrosion behavior of coating systems based on polyurethane and organic silicon compounds. *Prot. Met. Phys. Chem. Surf.* **2021**, *57*, 1034–1039. [CrossRef]
49. Taggart, O. A Study of the Mechanical Properties of Silicon-based Thin Films Deposited by ECR-PECVD and ICP-CVD. PhD Thesis, McMaster University, Hamilton, Ontario, 2013.
50. Angelini, E.; d'Agostino, R.; Fracassi, F.; Grassini, S.; Rosalbino, F. Surface analysis of PECVD organosilicon films for corrosion protection of steel substrates. *Surf. Interface Anal.* **2002**, *34*, 155–159. [CrossRef]
51. Carpentier, J.; Grundmeier, G. Chemical structure and morphology of thin bilayer and composite organosilicon and fluorocarbon microwave plasma polymer films. *Surf. Coat. Technol.* **2005**, *192*, 189–198. [CrossRef]
52. Babaei, S.; Profili, J.; Al Rashidi, M.; Dorris, A.; Beck, S.; Asadollahi, S.; Sarkassian, A.; Stafford, L. Permeation properties of a plasma-processed organosilicon-carboxymethylcellulose bilayer on fibrillated cellulosic films for sustainable packaging applications. *Cellulose* **2023**. *submitted*.
53. FDA. *Preparation of Premarket Submissions for Food Contact Substances (Chemistry Recommendations)*; Food and Drug Administration: Silver Spring, MD, USA, 2007.
54. Babaei, S.; Profili, J.; Asadollahi, S.; Sarkassian, A.; Dorris, A.; Beck, S.; Stafford, L. Analysis of transport phenomena during plasma deposition of hydrophobic coatings on porous cellulosic substrates in plane-to-plane dielectric barrier discharges at atmospheric pressure. *Plasma Process. Polym.* **2020**, *17*, 105865. [CrossRef]
55. Profili, J.; Levasseur, O.; Koronai, A.; Stafford, L.; Gherardi, N. Deposition of nanocomposite coatings on wood using cold discharges at atmospheric pressure. *Surf. Coat. Technol.* **2017**, *309*, 729–737. [CrossRef]
56. Profili, J.; Asadollahi, S.; Vinchon, P.; Dorris, A.; Beck, S.; Sarkassian, A.; Stafford, L. Recent progress on organosilicon coatings deposited on bleached unrefined Kraft paper by non-thermal plasma process at atmospheric pressure. *Prog. Org. Coat.* **2020**, *147*, 105865. [CrossRef]

57. HPFB. Information Requirements for Food Packaging Submissions. Available online: https://www.canada.ca/en/health-canada/services/food-nutrition/legislation-guidelines/guidance-documents/information-requirements-food-packaging-submissions.html (accessed on 7 February 2023).
58. Kuorwel, K.K.; Cran, M.J.; Orbell, J.D.; Buddhadasa, S.; Bigger, S.W. Review of mechanical properties, migration, and potential applications in active food packaging systems containing nanoclays and nanosilver. *Compr. Rev. Food Sci. Food Saf.* **2015**, *14*, 411–430. [CrossRef]
59. Brown, F.; Diller, K.R. Calculating the optimum temperature for serving hot beverages. *Burns* **2008**, *34*, 648–654. [CrossRef]
60. *OriginPro, Version 2015*; OriginLab Corporation: Northampton, MA, USA, 2015.
61. Hegemann, D.; Brunner, H.; Oehr, C. Plasma treatment of polymers to generate stable, hydrophobic surfaces. *Plasmas Polym.* **2001**, *6*, 221–235. [CrossRef]
62. Rahmati, S. Direct Rapid Tooling. In *Comprehensive Materials Processing*; Hashmi, S., Ed.; Elsevier: Amsterdam, Netherlands, 2014.
63. Busnel, F.; Blanchard, V.; Prégent, J.; Stafford, L.; Riedl, B.; Blanchet, P.; Sarkissian, A. Modification of sugar maple (acer saccharum) and black spruce (picea mariana) wood surfaces in a dielectric barrier discharge (DBD) at atmospheric pressure. *J. Adhes. Sci. Technol.* **2010**, *24*, 1401–1413. [CrossRef]
64. Stuart, S. *Organosilicon Chemistry: Special Lectures Presented at the International Symposium on Organosilicon Chemistry*; Elsevier: Amsterdam, Netherlands, 1966. [CrossRef]
65. Durbin, R.P. Osmotic flow of water across permeable cellulose membranes. *J. Gen. Physiol.* **1960**, *44*, 315–326. [CrossRef]
66. Mahomed, A.; Hukins, D.W.; Kukureka, S.N. Swelling of medical grade silicones in liquids and calculation of their cross-link densities. *Med. Eng. Phys.* **2010**, *32*, 298–303. [CrossRef] [PubMed]
67. Asadollahi, S.; Profili, J.; Farzaneh, M.; Stafford, L. Development of organosilicon-based superhydrophobic coatings through atmospheric pressure plasma polymerization of HMDSO in nitrogen plasma. *Materials* **2019**, *12*, 219. [CrossRef]
68. Pulpytel, J.; Kumar, V.; Peng, P.; Micheli, V.; Laidani, N.; Arefi-Khonsari, F. Deposition of organosilicon coatings by a non-equilibrium atmospheric pressure plasma jet: Design, analysis and macroscopic scaling law of the process. *Plasma Process. Polym.* **2011**, *8*, 664–675. [CrossRef]
69. Denton, P. 47—The water absorption characteristics of monofilament cellulose. *J. Text. Inst. Trans.* **1956**, *47*, T570–T585. [CrossRef]
70. Minelli, M.; Baschetti, M.G.; Doghieri, F.; Ankerfors, M.; Lindström, T.; Siró, I.; Plackett, D. Investigation of mass transport properties of microfibrillated cellulose (MFC) films. *J. Membr. Sci.* **2010**, *358*, 67–75. [CrossRef]
71. Kirk, C.T. Quantitative analysis of the effect of disorder-induced mode coupling on infrared absorption in silica. *Phys. Rev. B Condens. Matter* **1988**, *38*, 1255–1273. [CrossRef]
72. Duncan, B.; Urquhart, J.; Roberts, S. *Review of Measurement and Modelling of Permeation and Diffusion in Polymers*; National Physical Laboratory: Teddington, UK, 2005.
73. Russell, S.P.; Weinkauf, D.H. Vapor sorption in plasma polymerized vinyl acetate and methyl methacrylate thin films. *Polymer* **2001**, *42*, 2827–2836. [CrossRef]
74. Tsige, M.; Grest, G.S. Interdiffusion of solvent into glassy polymer films: A molecular dynamics study. *J. Chem. Phys.* **2004**, *121*, 7513–7519. [CrossRef] [PubMed]
75. Doremus, R.H. Diffusion of water in silica glass. *J. Mater. Res.* **1995**, *10*, 2379–2389. [CrossRef]
76. Erlat, A.G.; Spontak, R.J. SiOx gas barrier coatings on polymer substrates: Morphology and gas transport considerations. *J. Phys. Chem. B* **1999**, *103*, 6047–6055. [CrossRef]
77. Li, K.; Meichsner, J. Gas-separating properties of membranes coated by HMDSO plasma polymer. *Surf. Coat. Technol.* **1999**, *116–119*, 841–847. [CrossRef]
78. Palaskar, S.; Kale, K.H.; Nadiger, G.S.; Desai, A.N. Dielectric barrier discharge plasma induced surface modification of polyester/cotton blended fabrics to impart water repellency using HMDSO. *J. Appl. Polym. Sci.* **2011**, *122*, 1092–1100. [CrossRef]
79. FDA. *Nonclinical Studies for the Safety Evaluation of Pharmaceutical Excipients*; Food and Drug Admistration: Silver Spring, MD, USA, 2005.
80. *ASTM D859-16(2021)e1*; Standard Test Method for Silica in Water. American Society for Testing and Materials: West Conshohocken, PA, USA, 2021.
81. Baner, A.; Brandsch, J.; Franz, R.; Piringer, O. The application of a predictive migration model for evaluating the compliance of plastic materials with European food regulations. *Food Addit. Contam.* **1996**, *13*, 587–601. [CrossRef] [PubMed]
82. Ma, Y.; Song, F.; Hu, Y.; Kong, Q.; Liu, C.; Rahman, M.A.; Zhou, Y.; Jia, P. Highly branched and nontoxic plasticizers based on natural cashew shell oil by a facile and sustainable way. *J. Clean. Prod.* **2020**, *252*, 119597. [CrossRef]
83. Reynier, A.; Dole, P.; Feigenbaum, A. Prediction of worst case migration: Presentation of a rigorous methodology. *Food Addit. Contam.* **1999**, *16*, 137–152. [CrossRef] [PubMed]